◆ Human Brain Mapping 21:257–270(2004) ◆

Functional Coupling of Simultaneous Electrical and Metabolic Activity in the Human Brain

Terrence R. Oakes,[1]* Diego A. Pizzagalli,[2] Andrew M. Hendrick,[3] Katherine A. Horras,[3] Christine L. Larson,[3] Heather C. Abercrombie,[3] Stacey M. Schaefer,[3] John V. Koger,[3] and Richard J. Davidson[1,3,4]

[1]*W.M. Keck Laboratory for Functional Brain Imaging and Behavior, University of Wisconsin-Madison, Madison, Wisconsin*
[2]*Department of Psychology, Harvard University, Cambridge, Massachusetts*
[3]*Department of Psychology, University of Wisconsin-Madison, Madison, Wisconsin*
[4]*Department of Psychiatry, University of Wisconsin-Madison, Madison, Wisconsin*

Abstract: The relationships between brain electrical and metabolic activity are being uncovered currently in animal models using invasive methods; however, in the human brain this relationship remains not well understood. In particular, the relationship between noninvasive measurements of electrical activity and metabolism remains largely undefined. To understand better these relations, cerebral activity was measured simultaneously with electroencephalography (EEG) and positron emission tomography using [^{18}f]-fluoro-2-deoxy-D-glucose (PET-FDG) in 12 normal human subjects during rest. Intracerebral distributions of current density were estimated, yielding tomographic maps for seven standard EEG frequency bands. The PET and EEG data were registered to the same space and voxel dimensions, and correlational maps were created on a voxel-by-voxel basis across all subjects. For each band, significant positive and negative correlations were found that are generally consistent with extant understanding of EEG band power function. With increasing EEG frequency, there was an increase in the number of positively correlated voxels, whereas the lower α band (8.5–10.0 Hz) was associated with the highest number of negative correlations. This work presents a method for comparing EEG signals with other more traditionally tomographic functional imaging data on a 3-D basis. This method will be useful in the future when it is applied to functional imaging methods with faster time resolution, such as short half-life PET blood flow tracers and functional magnetic resonance imaging. *Hum. Brain Mapp. 21:257–270, 2004.* © 2004 Wiley-Liss, Inc.

Key words: positron emission tomography; PET; FDG; brain imaging; source localization; LORETA; EEG; EEG frequency bands; γ rhythms

INTRODUCTION

It is currently understood that scalp surface electroencephalographic (EEG) recordings at any given scalp location reflect electrical signals conducted throughout the brain [Speckman et al., 1993]. Because the normal cellular mechanism underlying these signals requires the metabolism of glucose and an abundant supply of oxygen, the measured

Contract grant sponsor: NIMH; Contract grant number: MH40747, P50-MH52354, MH43454, K05-MH00875; Contract grant sponsor: Swiss National Research Foundation; Contract grant number: 81ZH-52864; Contract grant sponsor: "Holderbank"-Stiftung zur Förderung der wissenschaftlichen Fortbildung; Contract grant sponsor: NRSA; Contract grant number: F31-MH12085.

*Correspondence to: Terrence R. Oakes, PhD, W.M. Keck Laboratory for Functional Brain Imaging and Behavior, T-133 Waisman Center, 1500 Highland Ave., Madison, WI 53705.
E-mail: oakes@falstaff.wisc.edu

Received for publication 31 July 2002; Accepted 5 November 2003
DOI 10.1002/hbm.20004

EEG signal is assumed to be closely related to the underlying spatio-temporal pattern of metabolism in the normal human brain [Ingvar et al., 1976, 1979; Nagata, 1988]; however, this relation is poorly understood. Several factors contribute to an ill-defined link. First, it is only recently that localization methods have been developed that permit a moderately accurate estimation of the sources within the brain for the electrical signals giving rise to observed surface EEG recordings. Second, the different frequency bands that comprise the signals are associated with different brain states, so regions of high metabolism are likely to be differentially associated with various EEG band power signals. Third, an electrical signal operates over a period of milliseconds, whereas the processes associated with noninvasive measurable changes in brain metabolism and hemodynamic function operate over a period of one to many seconds. Fourth, it is only recently that experiments have been conducted that reveal the relationship between electrical activity and metabolism on a cellular level in sufficient detail to permit hypotheses about the metabolic demands of neuroelectrical processes relevant to noninvasive imaging techniques [Logothetis et al., 2001; Mathieson et al., 1998].

The development of methods to measure regional cerebral blood flow (rCBF) and metabolism in vivo enabled researchers to combine EEG measurements with other measures of neuronal activity. These methods include the original nitrous oxide method to measure CBF [Kety and Schmidt, 1945] and metabolism via oxygen consumption [Kety and Schmidt, 1948], glucose consumption using positron emission tomography (PET) with the tracer [^{18}F]-fluoro-2-deoxy-D-glucose (FDG) [Phelps et al., 1979], and blood flow using magnetic resonance imaging (MRI) signal [Ogawa et al., 1990]. Early dual-modality studies [e.g., Obrist et al., 1963] did not attempt to localize either the EEG or CBF signal, but rather considered only the relationship of the overall EEG activity for a given frequency range to a global measure of blood flow or metabolism in the entire brain (or at best in each hemisphere). Improvements in methodology and technology permitted the testing of increasingly more specific hypothesis in subsequent work, as the locations of the underlying sources for metabolism/blood flow signals were improved using PET [Celesia et al., 1982; Danos et al., 2001; Hofle et al., 1997; Larson et al., 1998; Nagata, 1988; Nakamura et al., 1999; Sadato et al., 1998] and functional MRI (fMRI) [Goldman et al., 2002; Singh et al., 2003]. Parallel improvements in EEG technology and increased computational power led to improved localization of surface signals through more electrodes, more accurate modeling of electrical source location within the brain, and more accurate modeling of the time profile of single spike events.

The vast amount of data acquired in a standard neuroimaging study is reduced typically to a few local, contiguous regions of activation. An increase or decrease in measured signal in a local region compared to a baseline state is frequently interpreted as an increase (activation) or decrease (deactivation) in metabolism. Raichle et al. [2001] propose a definition for a baseline or resting state of cerebral metabolism as a state that yields a uniform oxygen extraction fraction (OEF) throughout the brain. In that work and a subsequent review article [Gusnard and Raichle, 2001], these authors point out that the brain is always active, and that activation or deactivation related to mental tasks or stimuli are merely changes from this well-defined baseline state. On a cellular level, Mathieson et al. [1998] suggest that both inhibitory and excitatory signals can contribute to an increase in rCBF, not only in the region producing the inhibitory/excitatory signals but also in the region receiving them. Efforts to model the relationship of cellular spiking and synaptic activity to the blood flow signal, typically measured with PET or fMRI [Almeida et al., 2002], provide a theoretical basis of support for these observations that contradict the notion that an excitatory signal must always be related to an increase in metabolism, and conversely that inhibitory signals must yield a deactivation. EEG measurements thus can be the result of either an inhibitory or an excitatory signal, and the related metabolic or rCBF signal can either increase or decrease. This is not a random process, however, and the expectation is that the same relationship will hold between electrical and metabolic signal for repeated measurements of the same state.

Recently, exciting advances have been made in understanding the relationship between electrical activity in the brain and the underlying metabolism that permits this activity. Ensembles of individual neurons act in synchrony to produce an electric field detectable via EEG measurements; specifically, it is the postsynaptic neuronal activity (as opposed to axonal spiking) that produces an EEG signal [Speckman et al., 1993]. In their work on the rat cerebellar cortex, Mathieson et al. [1998] found "a strong correlation between the product of field potential amplitude and stimulus frequency and CBF." Recent findings by Logothetis et al. [2001] "suggest that [blood oxygenation level-dependent] BOLD activation may actually reflect more the neural activity related to the input and the local processing in any given area, rather than the spiking activity commonly thought of as the output of the area." The EEG signal and metabolism/rCBF measurements (i.e., PET, fMRI) thus seem based on the same neurophysiologic phenomenon, namely local postsynaptic neuronal activity, and it is reasonable to expect that measures of brain electric and metabolic activity will be related in some fashion.

Although EEG signals typically have multiple components spread over a range of frequencies, and occur over a small fraction of the time required to obtain a single image using PET or functional MRI, it is clear from human studies that different EEG frequencies can be associated with specific spatial patterns in the brain that depend on mental state and activity of the subject, and that the EEG signal from various frequency bands can be correlated to underlying metabolism [Nagata et al., 1988].

Several recent studies have demonstrated a link between EEG signal and metabolism or blood flow. For example, Hofle et al. [1997] examined the relationship between rCBF and absolute EEG activity for the δ band during various

stages of sleep by carrying out an analysis of covariance with PET-rCBF data on a voxel-wise basis, using EEG δ activity obtained during the PET study as a covariate. Negative correlations were found between δ activity and rCBF in the thalamus and, to a lesser extent, in several other brain regions, whereas positive correlations were found in the visual and auditory cortex.

Several recent studies have examined the relationship between metabolism/rCBF and the α rhythm. Typically, EEG frequencies in the α band (8–12 Hz) are greatest in amplitude when subjects are in an awake, relaxed state with eyes closed. The α rhythm is thus a relatively easy phenomenon to induce and modulate in an experimental setting. Using a similar approach to that of Hofle et al. [1997], PET-rCBF was compared to EEG α [Sadato et al., 1998] and β [Nakamura et al., 1999] rhythms by averaging the EEG signal from the posterior scalp region and calculating the mean amplitude in each frequency band over the duration of the PET scan (90 sec). After spatially averaging the amplitude over all electrodes of interest, the resulting temporally and spatially averaged amplitude was used as a covariate to create a statistical parametric map using the *SPM* software package (Wellcome Department of Cognitive Neurology, London, UK). For normal subjects in a passive state [Sadato et al., 1998], a negative correlation was found between rCBF and α power in the occipital cortex, whereas positive correlations with α power were found in the pons, midbrain, hypothalamus, amygdala, basal prefrontal cortex, insula, and the right dorsal premotor cortex. For normal subjects listening to music [Nakamura et al., 1999], a positive correlation of posterior β power with rCBF was found in the premotor cortex and adjacent prefrontal cortices bilaterally, the anterior portion of the precuneus, and the anterior cingulate cortex in both rest and music conditions. In another study, Danos et al. [2001] correlated α power from EEG signal in electrodes over the occipital cortex with glucose metabolic rate (measured with PET-FDG) obtained from regions-of-interest (ROIs) in the occipital cortex and thalamus. In normal controls, positive correlations between α power and FDG metabolism were found in the right and left lateral thalamus, and a negative correlation was found in the left occipital cortex. In schizophrenic patients, however, no significant correlations between PET-FDG and EEG-α were found in these regions.

Goldman et al. [2002] simultaneously measured fMRI and EEG signals, focusing on the α rhythm, and found that in 11 normal subjects in a resting, eyes-closed state, "increased alpha power was correlated with decreased MRI signal in multiple regions of occipital, superior, inferior frontal, and cingulate cortex, and with increased signal in the thalamus and insula." Singh et al. [2003] studied the effect of stimulus frequency on the human visual system using EEG and fMRI with a flashing checkerboard experiment. In serial experiments, they found a strong correlation between EEG signal in two occipital electrodes and the fMRI (BOLD) signal in a large area that included the occipital cortex. In particular, there was a strong correlation between the two modalities for response magnitude related to variations in flashing frequency. Work in our laboratory has examined relations between EEG α power averaged over the entire head and glucose metabolism in the thalamus measured with PET-FDG [Larson et al., 1998], and found an inverse correlation between these measures in control subjects but not in a matched group of depressed subjects [Lindgren et al., 1999]. The studies summarized above represent a range of specificity with regard to spatial localization of various modalities; however, none of them examine correlations between flow or metabolism and electrophysiologic data at a specific tomographic location (i.e., on a voxel-wise basis).

In general, there are several major goals related to combining EEG and metabolism measures: (1) to investigate basic relationships between brain metabolism and electrical activity; (2) to deduce the generator or source location within the brain of various EEG frequencies; (3) to use metabolic activation locations as "seeds" for modeling the locations of EEG dipole sources; and (4) to combine the high temporal resolution of EEG with the spatial information obtained from a more traditional tomographic imaging modality to infer causal relationships of spatially distant activations.

The goal of the present work is to develop methodology for comparison of PET-FDG data and EEG data on a voxel-by-voxel basis. This requires tomographic source localization of the surface-based EEG data. There are multiple approaches to this problem [Baillet et al., 2001; Bosch-Bayard et al., 2001; Gorodnitsky et al., 1995]; based on previous work in our laboratory [e.g., Pizzagalli et al., 2001, 2002a], we selected the low-resolution electromagnetic tomography (LORETA) algorithm [Pascual-Marqui, 1999; Pascual-Marqui et al., 1994, 2002]. From the scalp-recorded electrical potential distribution, LORETA computes the 3-D intracerebral distributions of current density for specified EEG frequency bands. LORETA makes three major assumptions in estimating the source location of electrical activity: (1) that adjacent neurons act in synchrony, so that the activation distribution can be modeled as a smoothly varying field; (2) that the smoothest activity distribution is the most plausible; and (3) that the signal measured at the brain surface does not emanate from white matter or from certain subcortical structures deep in the brain. The latter assumption constrains the solution space of electrical activity to a standard brain template containing only cortical gray matter and the hippocampus; this template can then be used as a common space for comparing EEG data with data from another modality such as PET.

Although brain metabolism and electrical signal are related closely, the technical details of measuring one or the other of these aspects of brain function can differ greatly, as can the subsequent results. When EEG data are acquired during the first 30 min of the FDG uptake into the brain, the two modalities reflect the same brain state, even though the actual PET scan occurs after the EEG measurement. A resting PET-FDG study measures the basal metabolism of the brain during the uptake period of the FDG tracer, with the

bulk of the tracer uptake occurring in the first 30 min. Such PET data thus integrate brain metabolism over a relatively long time period, with poor temporal resolution but excellent chemical sensitivity and a reasonable spatial resolution. Different regions of the brain seem to contain neurons that fire or oscillate at different frequencies, and intriguingly, there seems to be electrophysiologic differences between some of these groups [Steriade et al., 1990] that may be manifested in differences in metabolic rate. EEG measurements reflect a range of frequency bands that are associated with various functional brain states [Basar et al., 1997; Davidson et al., 2000a; Klimesch, 1999; Schacter, 1977], and although EEG has relatively poor spatial resolution, it may be used to examine brain electrical activity on a time-scale of milliseconds. PET-FDG data are a composite or integral of the activity from all of the EEG bands, but it is unclear how the signal of each EEG band relates to the overall metabolism at a particular location.

There were two major purposes for the present study. First, abundant evidence from our laboratory has established that there are reliable individual differences in resting baseline parameters of brain electrical activity from prefrontal scalp regions that predict affective style [for review, see Davidson, 2000; Davidson et al., 2000b]. The fact that such associations have been established and replicated by other groups [e.g., Harmon-Jones and Allen, 1997; Wiedemann et al., 1999] underscores the need to identify better the intracerebral sources that give rise to these surface brain electrical events. The method featured in this study is suited ideally to this purpose because the previous studies have all been based on baseline resting measurements that are presumed to be replicable. Second, the analytic strategy developed for this study provides a methodology for comparing locations of metabolic activations and electrical activity sources using current noninvasive measurement techniques suitable for use with normal human subjects.

SUBJECTS AND METHODS

Subjects

Twelve right-handed normal subjects were recruited and tested in accord with procedures approved by the UW-Madison Human Subjects Committee. Each subject signed a consent form approved by this committee. Subjects ranged in age from 21–57 years (mean age, 35 ± 11.6 years), with six males and six females.

Experimental Procedures

The data analyzed in this work were acquired as part of a larger study investigating major depression, where the primary data of interest were the basal metabolisms obtained via the FDG-PET measurement [Abercrombie et al., 1998; Lindgren et al., 1999]. The acquisition protocol reflects this interest, and hence was not optimized for the EEG/PET comparison, which is the subject of the present study. PET data were recorded between 11:00 AM and 1:30 PM. After electrode application, preparations for the PET procedure were made, including the insertion of intravenous lines in the left hand (for blood sampling) and right arm (for radiotracer injection). Blood samples were withdrawn to obtain a radioactivity time-activity curve. EEG data collection began at the time of the FDG injection. The EEG data were acquired in a standard manner as detailed in Davidson et al. [2000a], with 10 contiguous 3-min trials to cover the first 30 min of radiotracer uptake. Verbal instructions to open or close eyes were given before the start of each trial, with an alternating order counterbalanced across participants. Alternating eyes-open and eyes-closed trials were chosen to conform to previous studies of baseline EEG asymmetry, where it was found that aggregating across eyes-open and eyes-closed trials gave the most reliable estimates of activation asymmetry [Tomarken et al., 1992], which was one of the main interests in acquiring these data. Upon completion of the 10 trials, electrodes and intravenous lines were removed.

EEG data acquisition

A modified Lycra electrode cap (Electro-Cap International, Inc.) with tin electrodes was used to record EEG from 28 scalp sites of the 10/10 system (FP1/2, F3/4, F7/8, FC3/4, FC7/8, C3/4, CP3/4, CP5/6, T3/4, T5/6, P3/4, PO3/4, FPz, Fz, Cz, Pz) referenced to the left ear (A1). Horizontal electrooculogram (EOG) was recorded from the external canthi of each eye and vertical EOG from the supra- to suborbit of one eye. Electrode impedances were under 5 KΩ for EEG (homologous sites within 2 KΩμ) and under 20 KΩ for EOG. Physiological signals were amplified with a Grass Model 12 Neurodata system using Model 12C preamplifiers (1–300 Hz bandpass with 60-Hz notch filter) and low pass filtered at 100 Hz. Analog signals were digitized on-line at 250 Hz.

PET-FDG scan

Subjects fasted for at least 5 hours before injection. Blood was sampled from an arterialized venous site [McGuire et al., 1976; Phelps et al., 1979] on the left hand for 30 min after injection. A population-averaged FDG blood curve was scaled to each subject's measured blood curve for the time period from 30 min after injection to the end of the PET scan. After voiding the bladder, the subjects were positioned on the scanner bed. PET data were acquired using a General Electric/Advance PET scanner [DeGrado et al., 1994]. This scanner has an intrinsic resolution of 5–6 mm full-width at half-maximum (FWHM), and a reconstructed resolution of 8–10 mm FWHM for a brain positioned near the center of the field of view. The scan started approximately 50 min after injection, and consisted of a 30-min 2D scan, a 10-min 3-D scan, and a 10-min transmission scan. The 2D PET data were reconstructed using the scanner manufacturer's software with calculated attenuation correction to 1.75 × 1.75 × 4.25 mm voxels, and converted to parametric images of an influx constant (K_i, 1/sec) according to a variation [Phelps et al., 1979] of the Sokoloff method [Sokoloff et al., 1977] for measuring the local cerebral metabolic rate of glucose consumption.

Data Analysis

EEG data

After off-line artifact rejection, non-overlapping 2,048-msec EEG epochs were extracted. After re-referencing to an average reference, all eyes-closed and eyes-open EEG epochs were analyzed with LORETA, which used a three-shell spherical head model [Ary et al., 1981] registered to the MNI-305 brain atlas [Collins et al., 1994; Evans et al., 1993] from the Brain Imaging Centre of the Montreal Neurologic Institute (referred to here as MNI coordinate space). EEG electrode coordinates were derived using cross-registrations between spherical and realistic head geometry [Towle et al., 1993]. The LORETA developer (Dr. Pascual-Marqui) provided a version of the software that is able to utilize up to 256 electrodes (28 electrodes were used in this study). Computations were restricted to cortical gray matter and hippocampi using the digitized probability atlases of the Montreal Neurologic Institute. If the probability of a voxel being gray matter was higher than 33% and higher than the probability of being white matter or cerebrospinal fluid, that voxel was labeled as gray matter. The solution space contained 2,394 voxels, each with a $7 \times 7 \times 7$ mm size. The spatial resolution of LORETA is estimated to be 1–2 voxels [Pascual-Marqui et al., 2002; and personal communication], or approximately 10 mm isotropically. Pascual-Marqui et al. [2002] use spatial dispersion as a metric for spatial resolution; although this is somewhat different from the FWHM metric commonly used in PET, we treat it as a FWHM value for the purpose of inter-modality comparison. The LORETA analyses consisted of two steps. First, for every subject, all available artifact-free 2,048-msec EEG epochs were subjected to cross-spectrum analysis via discrete Fourier transform (boxcar windowing) for the following EEG bands: θ (6.5–8.0 Hz), α1 (8.5–10.0 Hz), α2 (10.5–12.0 Hz), β1 (12.5–18.0 Hz), β2 (18.5–21.0 Hz), β3 (21.5–30.0 Hz), and γ (36.5–44.0 Hz). Second, LORETA computed current density as the linear weighted sum of the scalp electrical potentials and then squared this value for each voxel to yield power of current density.

PET data

The FDG-PET data were resampled to match the tomographic EEG data. First, the PET images were spatially normalized with *SPM99* [Friston et al., 1994] to the same coordinate space as that used by LORETA (MNI-305), and the validity of coregistration and smoothing was visually verified for each subject. FDG data were converted to $2 \times 2 \times 2$ mm voxels upon reslicing, and smoothed with a $6 \times 6 \times 6$ mm Gaussian kernel to approximate the estimated spatial resolution of LORETA (~10 mm). Using in-house software, the PET data were resampled to yield voxels with the same size and center location as the LORETA voxels. For this step, weighting factors for each PET voxel were used, derived by the fractional volume of a PET voxel that was completely or partially within a given LORETA voxel. To match the LORETA solution space, voxels not considered by LORETA were excluded from the resampled PET data. For all operations after the initial conversion to parametric influx-rate images, the PET units were maintained as μg/min/100 cc.

Statistical Analysis

Global correlations

Spearman's rank correlation coefficients (ρ) were calculated between the PET average metabolic activity (restricted to the voxels considered by LORETA) and the average current density estimate across all voxels for each EEG frequency band. To establish the validity of the Spearman's test with regard to this data set, a Shapiro-Wilk test was carried out across subjects for the global activity in each band of the LORETA data. Furthermore, the Shapiro-Wilk test was computed for 60 randomly selected voxels across all EEG bands to test whether values were distributed normally across subjects.

Voxel-wise correlations

A Spearman's rank correlation coefficient between PET and LORETA data was calculated for every valid LORETA voxel across all 12 subjects. We selected the Spearman's rank test because the distribution of values was not distributed normally, and in fact was different between the two modalities as well as among EEG frequency bands. The correlation coefficients were converted to a 3-D parametric map for visual inspection. For each band, the number of correlations associated with $P < 0.05$ (uncorrected for multiple comparisons) and $P < 0.01$ (uncorrected) were tabulated to assess how changes in frequency affected the number of positively and negatively correlated voxels. We considered voxels with $P < 0.01$ (uncorrected) to be significant, based on previous work with LORETA data [Pizzagalli et al., 2002a] using a randomization technique to estimate the false-positive rate under the null hypothesis, which demonstrated that a threshold of $P < 0.01$ provided adequate protection against Type I errors. A color-coded map of the Spearman's correlation coefficients is shown in Figure 1 for $P < 0.05$. Although we only considered results that survived the $P < 0.01$ threshold to be significant, we used a more liberal threshold in Figure 1 to demonstrate the utility of this method for identifying potentially interesting areas that may warrant further analysis.

The brain region and MNI coordinates closest to specific significant results were determined based on the Structure-Probability Maps atlas [Lancaster et al., 1997]. Brodmann's area (BA) and region labels are provided by the LORETA software. For a specific MNI coordinate, LORETA first determines the nearest gray matter voxel using a lookup table created via the Talairach Daemon [Lancaster et al., 2000], and then estimates a conversion from MNI space to Talairach space [Talairach and Tournoux, 1988] using the transform method suggested by Brett [2002]. Because the Talairach voxels are large relative to the 1-mm accuracy of

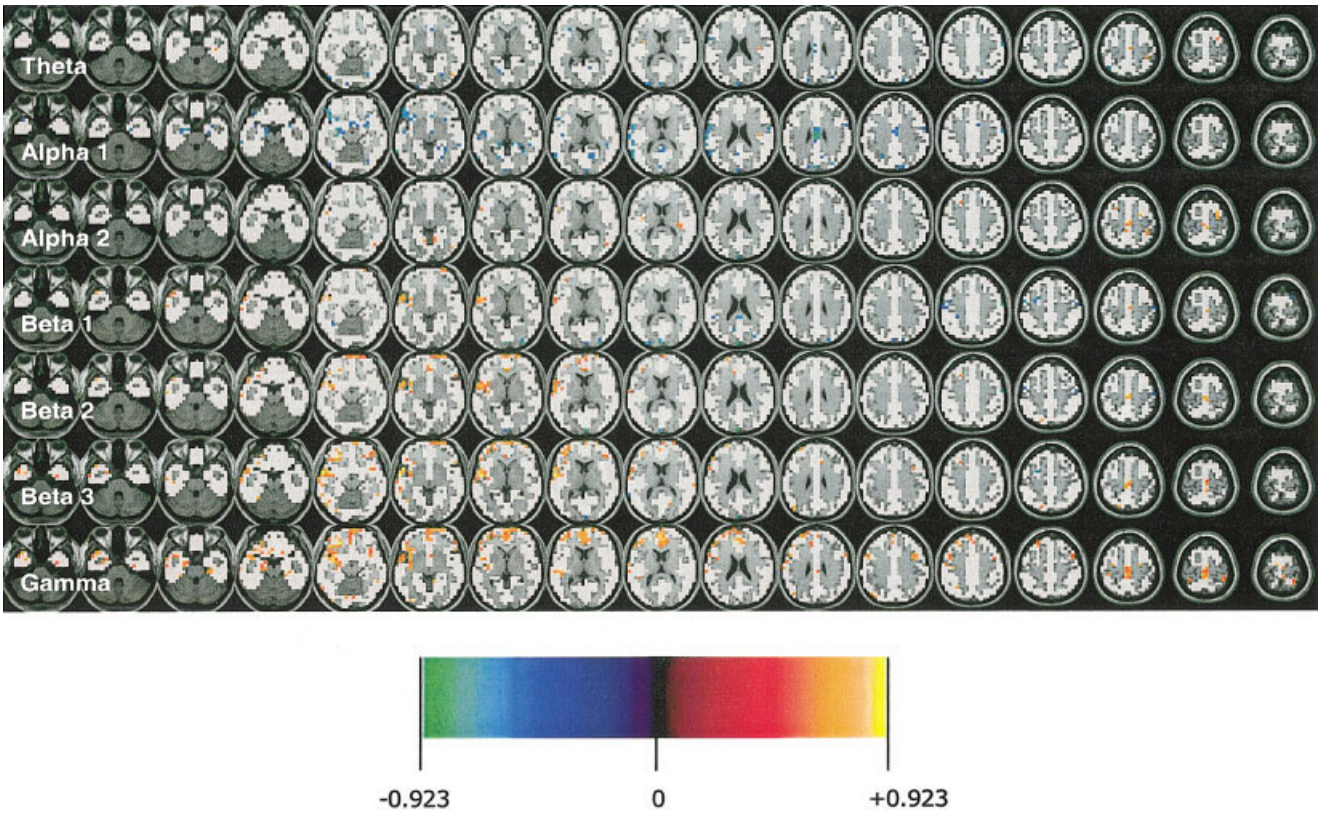

Figure 1.

Spearman's correlation maps between FDG-PET and EEG-LORETA (n = 12). The axial brain images go from inferior (**left**) to superior (**right**). Seven different EEG frequency bands are shown (one band per row): θ (6.5–8.0 Hz), α1 (8.5–10.0 Hz), α2 (10.5–12.0 Hz), β1 (12.5–18.0 Hz), β2 (18.5–21.0 Hz), β3 (21.5–30.0 Hz), and γ (36.5–44.0 Hz). The Spearman's correlation values are indicated by the color scale (**bottom**); all images use the same color scale, so all of the maps are directly comparable. The regions of the brain considered in the LORETA solution space but with greater uncertainty than the threshold ($P = 0.05$ uncorrected) are shown in light pink; the MRI image shows regions outside of the LORETA solution space.

the Talairach Daemon, there is occasionally some discrepancy between MNI coordinates and labels. The MNI coordinates given throughout this the present work are considered to be the true reference, whereas the labels are approximate.

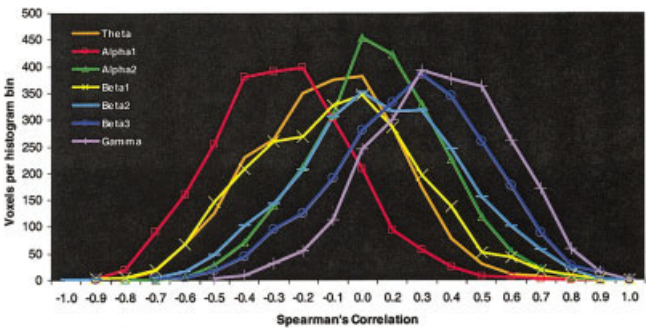

Figure 2.

Histograms of voxel-wise correlations between PET and each EEG frequency band.

Region-of-Interest Analysis

To examine the relationship between the intermodal Spearman's rank correlation and the relative signal intensity in a particular area, a region-of-interest (ROI) analysis was carried out. Two distinct locations with previously published findings linking metabolism and the α band were selected. For each ROI, the average value for all voxels within the region was calculated for each subject for both PET and LORETA data. The first region was the large cluster of negatively correlated voxels in the α1 band along the central axis (see Fig. 1, columns 11–12), comprised of 13 voxels (4.46 cm^3). The other region is in the occipital cortex (MNI coordinates $x = -46$ to $+45$, $y = -81$ to -95, $z = -13$), comprised of 28 voxels (9.60 cm^3). A global average was also calculated for all voxels within the LORETA solution space, and the ratio of ROI to global activity was calculated.

TABLE I. Correlations between global metabolic activity and average current density for seven EEG frequency bands

Band	Correlation (ρ)	*P*
θ	−0.252	0.430
α1	−0.378	0.226
α2	0.077	0.812
β1	−0.056	0.863
β2	0.189	0.557
β3	0.343	0.276
γ	0.483	0.112

Correlations (ρ) between global (averaged across voxels) metabolic activity and average current density for seven EEG frequency bands. The threshold for statistical significance is $P < 0.05$, $|\rho| > 0.591$.

RESULTS

Global Correlations

The correlations between global metabolic activity and average current density were uniformly low and nonsignificant for all EEG frequency bands (Table I), ranging from −0.378 to 0.483, ($P > 0.112$ in each of the seven bands). The low correlations between global FDG metabolism and average current density imply that subsequent voxel-wise correlations are due to regional effects rather than to an overall global effect. The results of the Shapiro-Wilk test for global activity show that the LORETA data are not distributed normally, and that a Spearman's test is appropriate. Furthermore, for the 60 randomly selected voxels, the Shapiro-Wilk test found that 51 of 60 voxels were significant, which implies that the voxel-wise LORETA activity for the seven classic bands is also not distributed normally across subjects.

Voxel-wise Correlations

The voxel-wise correlations between glucose metabolism and current density are summarized in Figure 1 for seven classic EEG bands. There were large positive and negative correlations within each band, which were not spread randomly throughout the brain, but rather tended to appear in spatially related clusters. Furthermore, there were pronounced regional variations of correlation coefficients among the various bands, with each band having a distinct pattern of clusters and isolated significant voxels. The lower-frequency bands (θ and α1) showed a low or negative correlation with respect to the PET data. As frequency increased, there was an increase in positive correlation between the modalities.

The correlation coefficients in Figure 1 range from −0.923 to +0.888 ($P < 0.001$). The locations of the minimum (negative correlation) and maximum (positive correlation) Spearman's correlation coefficients are shown in Table II, together with the location (MNI coordinates) of that voxel, the mean correlation value of all voxels in that band, and a description of the corresponding Brodmann's area and structure. The distribution of the coefficients in each band is shown in Figure 2. In general, correlations within each band are not distributed normally around zero, and the peak of each of the histograms varies from band to band.

TABLE II. Correlations across all LORETA voxels, and maximum and negative correlations for each EEG frequency band

Band	Hertz	Mean (SD)	Values	ρ	*x*	*y*	*z*	BA	Region
θ	6.5–8.0	−0.070 (0.237)	Min	−0.713[a]	18	−88	36	19	Cuneus
			Max	0.674[a]	46	−74	−6	37	Inferior temporal gyrus
			Max	0.674[a]	−38	−4	15	13	Insula
α1	8.5–10.0	−0.223 (0.227)	Min	−0.846[b]	−3	−18	29	23	Cingulate gyrus
			Max	0.660[a]	39	−18	22	13	Insula
α2	10.5–12.0	0.092 (0.222)	Min	−0.731[a]	−3	−95	22	19	Cuneus
			Max	0.755[a]	46	−74	−6	37	Inferior temporal gyrus
β1	12.5–18.0	−0.040 (0.273)	Min	−0.825[b]	−3	−95	22	19	Cuneus
			Max	0.825[b]	−52	10	−13	38	Superior temporal gyrus
β2	18.5–21.0	0.106 (0.267)	Min	−0.923[b]	−3	−95	22	19	Cuneus
			Max	0.829[b]	−52	10	−13	38	Superior temporal gyrus
β3	21.5–30.0	0.210 (0.257)	Min	−0.804[b]	−3	−95	22	19	Cuneus
			Max	0.888[b]	−59	−4	−6	21	Middle temporal gyrus
γ	36.5–44.5	0.306 (0.227)	Min	−0.469	−24	−4	50	6	Middle frontal gyrus
			Max	0.888[b]	−24	38	−13	11	Middle frontal gyrus

x, y, z are MNI coordinates of minimum and maximum values. Negative *x* values, left side of the brain; positive *x* values, right side of the brain. Brodmann's area (BA) and anatomic region (Region) derived from the Talairach Daemon [Lancaster et al., 2000] after converting MNI to Talairach coordinates. BA and region denote the closest gray matter voxel to that location.
[a] $P < 0.05$ (uncorrected; $\rho > 0.591$); [b] $P < 0.01$ ($|\rho| > 0.727$).

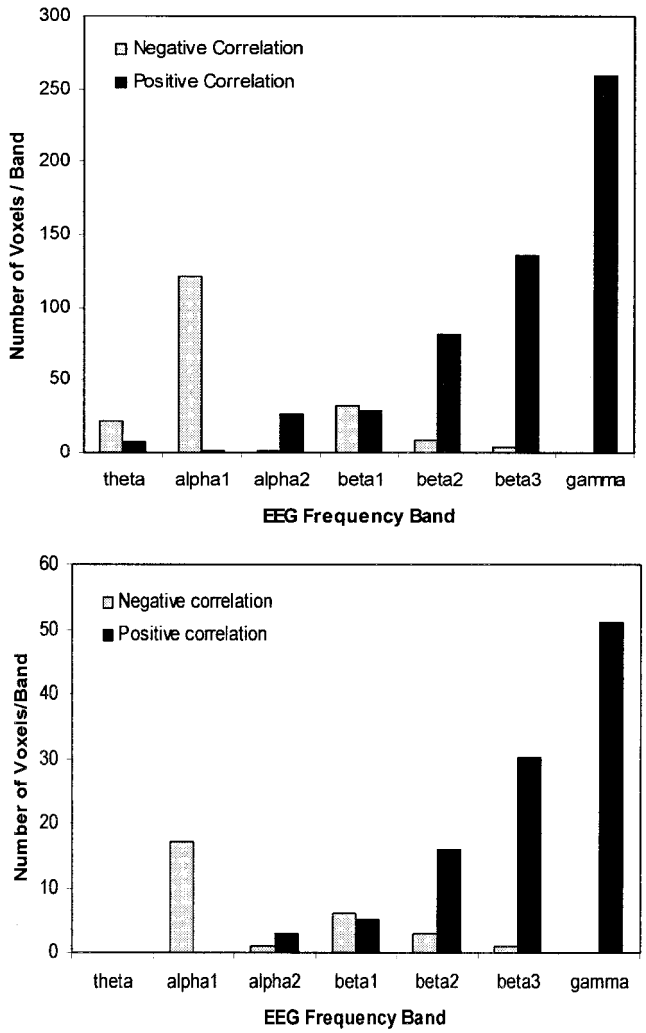

Figure 3.
Number of voxels from each EEG frequency band with a significance level (uncorrected) higher than $P = 0.05$ (**top**) and higher than $P = 0.01$ (**bottom**) for both negative and positive correlations.

The number of voxels in each EEG frequency band where the correlations had a significance higher than $P < 0.05$ (uncorrected, $|\rho| > 0.591$) and $P < 0.01$ (uncorrected, $|\rho| > 0.727$) are summarized in Figure 3. There was a systematic increase in the number of significant positive correlations with increasing frequency, whereas the largest number of significant negative correlations was found in the α1 band.

An important limitation of the current method (and any similar group-wise correlation) is that it does not indicate positive or negative correlations between the *activations* of two modalities. Rather, it indicates correlations between the voxel-wise *ranks* of individuals within each modality. For example, EEG may yield a uniformly low α-band activity in a particular voxel, and FDG-PET may show a fairly large metabolism in the same voxel, but a high correlation will result if the rank for each modality is similar. An example of this is demonstrated by the ratios and variances shown in Table III. The midline region showed an inverse correlation between PET and EEG measurements. An examination of the data values showed that the average LORETA value for all subjects in this ROI was less than half (0.471) the average value for the entire LORETA brain solution space, whereas the corresponding average PET ROI value was nearly three times (2.764) the average of the same whole-brain solution space. The difference between these two groups of ROIs was significant ($P < 10^{-9}$ for a paired *t*-means test), demonstrating that in this region the LORETA data were lower than average, whereas the PET data were higher than average. This is consistent with the assumption that α is inversely related to activation. In this example, the correlational data showed an inverse relation between modalities, but the ROI analysis was required to determine the modality that shows a higher signal relative to other brain regions.

A different situation emerged for the occipital cortex ROI: both the PET and the LORETA data in this region were two to three times higher than the brain solution space average, whereas the correlations between PET/FDG and EEG ranks were negative (although for most of the occipital ROIs this was not significant). This was an example of a region that had an increased signal compared to the global brain average in both modalities, yet yielded an inverse correlation between modalities. The finding of a higher than average signal for both metabolism and EEG/α1 seems inconsistent with the assumption that α is inversely related to activation. This example underscores the limitations of the eyes-open/eyes-closed paradigm of this particular data set, however, because α activity was associated with an eyes-closed resting state in this region, whereas the higher metabolism in the visual system in this area was most likely related to the eyes-open state. Because both states were present during the 30-min measurement period, both modalities showed signal increases in this area.

TABLE III. Mean and variance for LORETA and PET data across subjects for ratio of cluster/global activity in two regions of interest from the α1 band

Region	Modality	Mean	Variance	Variance/mean
Midline[a]	LORETA	0.471	0.016	0.0343
	PET	2.764	0.127	0.0459
Occipital cortex[b]	LORETA	2.307	0.043	0.0187
	PET	3.025	0.040	0.0133

[a] Midline region refers to a significant cluster along the midline, superior to the thalami (green cluster in Fig. 1, row 2, column 11).
[b] Occipital cortex region refers to the entire occipital cortex including nonsignificant voxels in MNI axial plane $z = -13$ (see Fig. 1, row 2, column 5).

DISCUSSION

The present study showcases a novel approach that permits comparison of concurrently measured EEG and PET data across a group of subjects. This method establishes that, depending on the EEG frequency band, there are distinct and localized regions within the brain where the modalities correlate. In general, higher EEG frequency bands contain more positively correlated regions, whereas lower EEG frequency bands contain more inversely correlated regions. Specifically, the α1 band (8.5–10.0 Hz) contains the largest number of inverse correlations, and the γ band (30.5–44.5 Hz) contains the largest number of positive intermodal correlations.

Because it is the correlation of the ranks of the values and not the values themselves that is examined in this method, further analysis is required to determine if the correlated voxels correspond to regions of high or low activity from either modality. More importantly, the neurophysiologic mechanisms underlying relations between activity in different EEG bands and metabolic activity need to be elucidated. In addition, it is important to point out that neither a high intermodal correlation nor a high metabolism signal necessarily means the area is activated. The region could, for example, simply have a higher basal metabolism. A comparison with a true baseline condition [Raichle et al., 2001] is required to determine if the region is in fact activated.

The approach adopted in this report depends on the accuracy of the EEG source estimation. There are two aspects that potentially limit this accuracy: the number of EEG electrodes, and the source estimation method. Recently, EEG systems comprised of 128 or more electrodes have become commonplace. Because the current work only utilized 28 electrodes, future studies that take advantage of denser electrode arrays can expect to realize greater localization accuracy, regardless of the source estimation method. The primary criticism of the LORETA source estimation algorithm used in this work is that, like other minimum-norm approaches, it over-smooths the extent of the activation [Fuchs et al., 1999; Koles, 1998], and the minimum-norm class of solutions to which LORETA belongs can yield erroneous solutions for sparsely sampled data sets [Baillet et al., 2001]. Simulations [Pascual-Marqui, 1999] have shown that if the underlying source distribution is "neurophysiologically smooth" then LORETA can localize it precisely; if not, the algorithm yields a blurred (low resolution) solution. Whereas some independent simulations [Fuchs et al., 1999] have suggested that the LORETA algorithm performs better than other linear algorithms (e.g., minimum norm least squares), others have raised considerable criticisms against it, particularly in cases of different sources with similar intensity but different eccentricities [Grave de Peralta Menendez and Gonzales Andino, 2000]. From an empirical perspective, several studies utilizing LORETA [Frei et al., 2001; Pascual-Marqui et al., 1999; Pizzagalli et al., 2000, 2001; Seeck et al., 1998; Worrell et al., 2000] have yielded results in agreement with known brain function. Furthermore, various independent studies have reported cross-modal validation between LORETA estimates and functional MRI [Seeck et al., 1998], structural MRI [Worrell et al., 2000], electrocorticography from subdural electrodes [Seeck et al., 1998], and PET [Pizzagalli et al., 2002b].

Unfortunately, we could not directly compare results between this study and two previous studies that examined the same data set [Larson et al., 1998; Lindgren et al., 1999], because the previous works reported correlations between PET and α activity in the thalamus, but the LORETA solution space does not include the thalamus. Larson et al. [1998] reported a robust inverse correlation between global α power and FDG metabolism in a region that included the thalamus for a group containing 19 depressed and 8 nondepressed (control) subjects. Lindgren et al. [1999] placed ROIs over each thalamus for a larger group of depressed and nondepressed subjects, and found a significant inverse correlation between global α power and FDG metabolic rate in the control but not the depressed group. The subjects of the current LORETA/FDG comparison include 12 of 13 control subjects used by Lindgren et al. [1999] (one subject was excluded due to technical difficulties with converting the data into the LORETA tomographic format). Not surprisingly, the results for the α1 band (see Fig. 1, columns 11–12) found a strong inverse correlation between EEG and FDG activity at a location near the thalamus, similar to the results of the voxel-wise correlation found by Larson et al. [1998] (Fig. 1) between FDG activity and α power: on the midline and superior to the thalami. This is actually the closest location within the LORETA search space to the average location of the thalami, and could represent a source of electrical activity that originated in the two thalami but which LORETA misplaced due to limited solution space. It is unfortunate that locations of deep gray-matter structures such as the thalamus, caudate, and putamen are not considered by LORETA; however, any electrical activity with a source location in these regions may still be measured by the EEG apparatus, and such a signal would have to be accounted for by LORETA. In this case, a misplaced thalamus signal is a possible result.

As seen in Table III for the midline region, this cluster has an average value in PET gray-matter that is nearly three times larger than the average value of the global solution space, whereas in the LORETA data the cluster is approximately half of the average α1 global electrical activity; thus, not only are the intermodal subject ranks in this region significantly inversely correlated, the relative signal intensity in the region is also inversely related: it has a relatively low LORETA α1 activity and a relatively high metabolism. This implies that this region is not a strong generator of α1 signal, although the experimental protocol with alternating blocks of eyes-open/eyes-closed limits this interpretation. A limited analysis (data not presented) for a single voxel from a randomly selected subject examining the time-course of the LORETA signal in the midline region (as defined in Table III) was unable to distinguish between eyes-open and eyes-closed, providing further evidence that the electrical

signal represented by this region is not associated with generation of α. Conversely, the occipital cortex region in Table III highlights a group of voxels whose ranks show a generally inverse correlation between the EEG and PET modalities, but whose relative signal intensities levels are similar: for both modalities this region is well above the average solution-space value. This underscores an important caveat in interpreting the results of any correlational analytic approach: regions with a high correlation across subjects need not have a correspondingly high activation in either of the two modalities.

In another study comparing EEG α power to FDG metabolism, Danos et al. [2001] found a significant negative correlation in the left occipital cortex. Although the spatial extent may be smaller in the current LORETA/FDG comparison, several voxels in the left and right occipital cortex yielded significant correlations in the same direction as found by Danos et al. [2001], who also found a significant positive correlation in the left and right lateral thalamus. Their study, however, examined correlations between PET/FDG in the thalamus and EEG/α using normalized and absolute power from four EEG leads located over the occipital cortex, with no attempt made to localize further the EEG signal to a particular region of the brain. On the other hand, the current work utilizes information from all electrodes to estimate the source location(s) of EEG signal, and performs a voxel-wise correlation between modalities. Danos et al. [2001] correlated metabolism in the thalamus with α power that was related most clearly to the occipital cortex, whereas the current study, with its voxel-wise correlation, attempts to relate metabolism and EEG activity at corresponding locations throughout the brain.

Sadato et al. [1998] simultaneously recorded EEG signals from the posterior one-third of the scalp while measuring rCBF using PET with [^{15}O]-H_2O as a tracer. They found a large region of negative correlation between α power and rCBF in the occipital cortex, and found several other regions with a positive correlation between EEG and rCBF. Unfortunately for the purposes of comparison with the present study, several of these regions, such as the midbrain and hypothalamus, are not in the LORETA solution space. Although the insula is implicated as the structure containing the maximal positive correlation in the present work for the α1 band and was a structure also found by Sadato et al. [1998] to be positively correlated, the comparison between the previous findings and the current work must be viewed with caution, as the insula coordinates provided by Sadato et al. [1998] are relatively far from the insula finding in the current work. Furthermore, the insula finding in the current work is limited to a single voxel in the α 1 band, and this voxel is located at the interior edge of the LORETA solution space, introducing the possibility of a mismatched LORETA location similar to that discussed above for the thalamus. A direct comparison between the work of Sadato et al. [1998] and the current work, however, is clouded further for the same reason as the comparison with the work of Danos et al. [2001] mentioned above; namely, Sadato et al. [1998] correlated voxel-wise metabolism with average α power from a group of posteriorly positioned electrodes, and did not attempt to localize the EEG activity to a particular location as in the current study. Furthermore, the tasks were quite different between these studies, and Sadato et al. [1998] took EEG measurements over a brief period of time 15 min after FDG injection, whereas the present study examined the EEG signal for the full 30 min after injection.

In recent work, Goldman et al. [2002] presented results obtained from simultaneous fMRI and EEG measurements, focusing on the α rhythm. They found that "increased α power was correlated with decreased MRI signal in multiple regions of occipital, superior temporal, inferior frontal, and cingulate cortex, and with increased signal in the thalamus and insula." Despite the limitations of LORETA to localize a signal in certain structures such as the thalamus, the current LORETA/FDG comparison found significant positive and negative correlations in most of these regions.

Goldman et al. [2002] point out a difference between their finding of a positive correlation between α power and fMRI signal in the thalamus, and a previous finding by Larson et al. [1998] and Lindgren et al. [1999] of an inverse correlation between α power and FDG metabolism in the same region. An explanation suggested by Goldman et al. [2002] is that, due to the extended data collection period during the FDG uptake period and the resulting poor temporal resolution, Larson et al. [1998] and Lindgren et al. [1999] were unable to examine phasic changes on an individual level. Goldman et al. [2002] then reasonably suggests that the extended time period may result in more trait-like properties of α generation, whereas the fMRI findings in their work may " …reflect α modulation on an individual subject level, and thus may highlight the role of the thalamus in moment-to-moment wave generation." The major differences between these two findings is related most likely to the duration of time of data collection: the short duration of acquisition in Goldman et al. [2002] reflects individual state features, whereas the relatively long acquisition duration of the current work likely reflects trait features.

Differences between the results of the current study and Goldman et al. [2002] may also be related to the difference in experimental design. The previous study examined subjects in a resting state with eyes closed, but the data set examined by the current work [and by Larson et al., 1998; Lindgren et al., 1999] alternated eyes-open with eyes-closed periods for the 30-min duration of the initial FDG uptake. Because the eyes-open and eyes-closed periods were pooled for PET and EEG measures, the strength of the α signal, which is strongest when a subject is awake with eyes closed, might not be expected to reach the full signal strength had the eyes been closed for the entire measurement period. Furthermore, there are likely to be confounding signals due to the combination of the two states, making it difficult to compare directly with data from a single state. The difference in subject state could also explain the discrepancy between findings of a positive correlation of α signal and FDG me-

tabolism in the thalamus by Danos et al. [2001], and the inverse result found in the current data set.

A limitation of the FDG tracer is that over the span of 30 min it is difficult to ensure that the subject remains in the same functional state, so that a variety of EEG signals and metabolic states may become temporally averaged. This averaging process occurs in the analysis process via a computer algorithm, and it is unlikely that the selected averaging scheme will match the average neuronal activity over the same 30 min. The sensitivity of an inter-modality correlation is thus diminished, and interpretation of results becomes less clear. An example of this may be seen in the results presented in Table III for a region in the occipital cortex. Typically, while the eyes are closed and the subject is awake, a larger than average signal is expected in this region in the α band compared to other states (e.g., eyes open). Because α activity is typically inversely correlated with brain activity, one might expect a lower than average PET signal in this area. The LORETA and PET data, however, show a 2.3- and 3-fold larger signal, respectively, in this area compared to the rest of the brain. This can be explained by several mechanisms. One explanation is that this could provide evidence for a region where α EEG activity is positively correlated with metabolism, although this does not fit with current understanding of the α signal. A more likely (and competing) explanation is related to the experimental protocol, which required the subjects to open and close their eyes for alternating 3-min blocks. The eyes-closed state would be expected to yield a strong α1 signal, whereas the eyes-open state would be expected to lead to increased metabolic activity in this region. This particular acquisition protocol thus seems poorly suited for the current cross-modality comparison, and was only used because this initial methodological development was undertaken using a previously existing data set.

A shorter-lived radiotracer such as [^{15}O]-H_2O, which measures blood flow, or simultaneous fMRI [Bonmassar et al., 2001; Goldman et al., 2000, 2002; Lazeyras et al., 2000; Lemieux et al., 2001; Schomer et al., 2000], would provide a better temporal match to the EEG data, permitting investigation of state parameters. Simultaneous fMRI or [^{15}O]-H_2O-PET would also permit a design with multiple conditions that could support a within-subject analysis approach, which would complement and extend the method used here. Because this study examined relations across rather than within subjects, it necessarily highlights the role of individual trait differences in baseline patterns of regional activation and their reflection in both EEG and PET. The goal of the original study from which the current data set was drawn was to examine individual trait differences. For this purpose, the relatively poor timing resolution of the current study can be a virtue, because a more stable estimate of trait parameters emerges from the extended data acquisition period.

The results presented in this methodologically oriented work are uncorrected for multiple comparisons. Although results surviving a Bonferroni correction for all voxels tested within the brain would be statistically irreproachable, this approach is considered too conservative for most neuroimaging data, which tend to have a fair amount of correlation between adjacent voxels. This is especially true for PET data, which are reconstructed from counts between detector pairs that view many voxels along the line connecting each pair, and also for LORETA data, where the smoothest solution is assumed to be the most likely. Less conservative alternatives to a strict Bonferroni correction include using a Monte Carlo simulation of the data to estimate the probability of a false-positive result [e.g., as implemented in AFNI; see Cox, 1996; Ward, 2000], using a nonparametric permutation approach [Nichols and Holmes, 2001], or using a parametric general linear model approach with corrections for multiple comparisons derived from random field theory [Friston et al., 1995; Worsley et al., 1992]. To apply the results of this inter-modality comparison method to a data set of physiologic interest, one of these or another appropriate correction for multiple comparisons would buttress the statistical validity of the results.

Despite the limitations noted above, the present results revealed robust associations between the PET and EEG data that are generally consistent with extant understanding of EEG phenomena. With increasing EEG frequency there was an increase in the number of positively correlated voxels, suggesting that for higher EEG frequencies more regions were coupled with higher regional glucose metabolism. In addition, the lower α band (8.5–10.0 Hz) was associated with the highest number of negative correlations, in agreement with the traditional view that this rhythm may be inversely related to brain activation [Davidson et al., 2000a; Shagass, 1972]. These findings may have important implications for studies that use EEG to derive a metric of activation and suggest that either α1 or γ band power be elected as inverse or direct measures of activation.

CONCLUSIONS

We present an approach for comparing brain electrical activity and cerebral glucose consumption within the same tomographic reference frame. A 3-D correlational map was created for each EEG frequency band with FDG-PET data across multiple subjects. Our findings revealed striking differences in the correlations between γ or α1 and glucose metabolism with the former showing positive and the latter showing inverse associations. Future studies with this multimodal integration approach that utilize hemodynamic measures with better time resolution than FDG-PET (e.g., fMRI or [^{15}O]-H_2O-PET) will be able to examine associations between task-elicited brain electrical and hemodynamic signals in a within-subject design.

ACKNOWLEDGMENTS

This work was supported by in part by the NIMH (Research Scientist Award K05-MH00875 to R.J.D., and MH40747, P50-MH52354, MH43454), the Swiss National Research Foundation (81ZH-52864 to D.A.P.), "Holderbank"-

Stiftung zur Förderung der wissenschaftlichen Fortbildung (D.A.P.), and by the NRSA (Predoctoral Fellowship Award F31-MH12085 to C.L.L.).

REFERENCES

Abercrombie HC, Schaefer SM, Larson CL, Oakes TR, Lindgren KA, Holden JE, Perlman SB, Turski PA, Krahn DD, Benca RM, Davidson RJ (1998): Metabolic rate in the right amygdala predicts negative affect in depressed patients. Neuroreport 9:3301–3307.

Almeida R, Stetter M (2002): Modeling the link between functional imaging and neuronal activity: synaptic metabolic demand and spike rates. Neuroimage 17:1065–1079.

Ary JP, Klein SA, Fender DH (1981): Location of sources of evoked scalp potentials: corrections for skull and scalp thicknesses. IEEE Trans Biomed Eng 28:447–452.

Baillet S, Riera JJ, Marin G, Mangin JF, Aubert J, Garnero L (2001): Evaluation of inverse methods and head models for EEG source localization using a human skull phantom. Phys Med Biol 46: 77–96.

Basar E, Schurmann M, Basar-Eroglu C, Karakas S (1997): α oscillations in brain functioning: an integrative theory. Int J Psychophysiol 26:5–29.

Bonmassar G, Schwartz DP, Liu AK, Kwong KK, Dale AM, Belliveau JW (2001): Spatiotemporal brain imaging of visual-evoked activity using interleaved EEG and fMRI recordings. Neuroimage 13:1035–1043.

Bosch-Bayard J, Valdes-Sosa P, Virues-Alba T, Aubert-Vazquez E, John ER, Harmony T, Riera-Diaz J, Trujillo-Barreto N (2001): 3-D statistical parametric mapping of EEG source spectra by means of variable resolution electromagnetic tomography (VARETA). Clin Electroencephalogr 32:47–61.

Brett M (2002): The MNI brain and the Talairach atlas. London: Medical Research Council. Online at http://www.mrc-cbu.cam.ac.uk/Imaging/Common/mnispace.shtml.

Celesia GC, Polcyn RD, Holden JE, Nickles RJ, Gatley JS, Koeppe RA (1982): Visual evoked potentials and positron emission tomographic mapping of regional cerebral blood flow and cerebral metabolism: can the neuronal potential generators be visualized? Electroencephalogr Clin Neurophysiol 54:243–256.

Collins DL, Neelin P, Peters TM, Evans AC (1994): Automatic 3-D intersubject registration of MR volumetric data in standardized Talairach space. J Comput Assist Tomogr 18:192–205.

Cox RW (1996): AFNI: software for analysis and visualization of functional magnetic resonance neuroimages. Comput Biomed Res 29:162–173.

Danos P, Guich S, Abel L, Buchsbaum MS (2001): EEG α rhythm and glucose metabolic rate in the thalamus in schizophrenia. Neuropsychobiology 43:265–272.

Davidson RJ (2000): Affective style, psychopathology and resilience: brain mechanisms and plasticity. Am Psychol 55:1196–1214.

Davidson RJ, Jackson DC, Larson CL (2000a): Human electroencephalography. In: Cacioppo JT, Tassinary LG, Bernston GG, editors. Handbook of psychophysiology: human electroencephalography. Cambridge: Cambridge University Press. p 27–56.

Davidson RJ, Jackson DC, Kalin NH (2000b): Emotion, plasticity, context and regulation: perspectives from affective neuroscience. Psychol Bull 126:890–906.

DeGrado TR, Turkington TG, Williams JJ, Stearns CW, Hoffman JM, Coleman RE (1994): Performance characteristics of a whole-body PET scanner. J Nucl Med 35:1398–1406.

Evans AC, Collins DL, Mills SR, Brown ED, Kelly RL, Peters TM (1993): 3-D statistical neuroanatomical models from 305 MRI volumes. Proc IEEE Nucl Sci Symp Med Imaging 95:1813–1817.

Frei E, Gamma A, Pascual-Marqui R, Lehmann D, Hell D, Vollenweider FX (2001): Localization of MDMA-induced brain activity in healthy volunteers using low resolution brain electromagnetic tomography (LORETA). Hum Brain Mapp 14:152–165.

Friston KJ, Worsley KJ, Frackowiak RSJ, Mazziotta JC, Evans AC (1994): Assessing the significance of focal activations using their spatial extent. Hum Brain Mapp 1:214–220.

Friston KJ, Holms AP, Worsley KJ, Poline JP, Frith CD, Frackowiak RSJ (1995): Statistical parametric maps in functional imaging: a general linear approach. Hum Brain Mapp 2:189–210.

Fuchs M, Wagner M, Köhler T, Wischmann HA (1999): Linear and nonlinear current density reconstructions. J Clin Neurophysiol 16:267–295.

Goldman RI, Stern JM, Engel J, Cohen MS (2000): Acquiring simultaneous EEG and functional MRI. Clin Neurophysiol 111:1974–1980.

Goldman RI, Stern JM, Engel J, Cohen MS (2002): Simultaneous EEG and fMRI of the α rhythm. Neuroreport 13:2487–2492.

Gorodnitsky IF, George JS, Rao BD (1995): Neuromagnetic source imaging with FOCUSS: a recursive weighted minimum norm algorithm. Electroencephalogr Clin Neurophysiol 95:231–251.

Grave de Peralta Menendez R, Gonzales Andino SL (2000): Discussing the capabilities of Laplacian minimization. Brain Topogr 13:97–104.

Gusnard DA, Raichle ME (2001): Searching for a baseline: functional imaging and the resting human brain. Nat Rev Neurosci 210: 685–694.

Harmon-Jones E, Allen JJB (1997): Behavioral activation sensitivity and resting frontal EEG asymmetry: covariation of putative indicators related to risk for mood disorders. J Abnorm Psychol 106:159–163.

Hofle N, Paus T, Reutens D, Fiset P, Gotman J, Evans AC, Jones BE (1997): Regional cerebral blood flow changes as a function of δ and spindle activity during slow wave sleep in humans. J Neurosci 172:4800–4808.

Ingvar DH, Sjolund B, Ardo A (1976): Correlation between dominant EEG frequency, cerebral oxygen uptake and blood flow. Electroencephalogr Clin Neurophysiol 41:268–276.

Ingvar DH, Rosen I, Johannesson G (1979): EEG related to cerebral metabolism and blood flow. Pharmakopsychiatr Neuropsychopharmakol 12:200–209.

Kety SS, Schmidt CF (1945): The determination of cerebral blood flow in man by the use of nitrous oxide in low concentrations. Am J Physiol 143:53–66.

Kety SS, Schmidt CF (1948): The nitrous oxide method for the quantitative determination of cerebral blood flow in man: theory, procedure and normal values. J Clin Invest 27:476.

Klimesch W (1999): EEG α and θ oscillations reflect cognitive and memory performance: a review and analysis. Brain Res 29:169–195.

Koles ZJ (1998): Trends in EEG source localization. Electroencephalogr Clin Neurophysiol 106:127–137.

Lancaster JL, Rainey LH, Summerlin JL, Freitas CS, Fox PT, Evans AC, Toga AW, Mazziotta JC (1997): Automated labeling of the human brain: a preliminary report on the development and evaluation of a forward-transform method. Hum Brain Mapp 5:238–242.

Lancaster JL, Woldorff MG, Parsons LM, Liotti M, Freitas CS, Rainey L, Kochunov PV, Nickerson D, Mikiten SA, Fox PT

(2000): Automated Talairach atlas labels for functional brain mapping. Hum Brain Mapp 10:120–131.

Larson CL, Davidson RJ, Abercrombie HC, Ward RT, Schaeffer SM, Jackson DC, Holden JE, Perlman SB (1998): Relations between PET-derived measures of thalamic glucose metabolism and EEG α power. Psychophysiology 35:162–169.

Lazeyras F, Blanke O, Zimine I, Delavelle J, Perrig SH, Seeck M (2000): MRI, ^{1}H-MRS, and functional MRI during and after prolonged nonconvulsive seizure activity. Neurology 55:1677–1682.

Lemieux L, Salek-Haddadi A, Josephs O, Allen P, Toms N, Scott C, Krakow K, Turner R, Fish DR (2001): Event-related fMRI with simultaneous and continuous EEG: description of the method and initial case report. Neuroimage 14:780–787.

Lindgren KA, Larson CL, Schaefer SM, Abercrombie HC, Ward RT, Oakes TR, Holden JE, Perlman SB, Benca RM, Davidson RJ (1999): Thalamic metabolic rate predicts EEG α power in healthy control subjects but not in depressed patients. Biol Psychiatry 45:943–952.

Logothetis NK, Pauls J, Augath M, Trinath T, Oeltermann A (2001): Neurophysiological investigation of the basis of the fMRI signal. Nature 412:150–157.

Mathieson C, Ceasar K, Akgören N, Lauritzen M (1998): Modification of activity-dependent increases of cerebral blood flow by excitatory synaptic activity and spikes in rat cerebellar cortex. J Physiology 512:555–566.

McGuire EAH, Helderman JH, Tobin JD, Andres R, Berman M (1976): Effects of arterial versus venous sampling on analysis of glucose kinetics in man. J Appl Physiol 41:565–573.

Nagata K (1988): Topographic EEG in brain ischemia—correlation with blood flow and metabolism. Brain Topogr 1:97–106.

Nakamura S, Sadato N, Oohashi T, Nishina E, Fuwamoto Y, Yonekura Y (1999): Analysis of music-brain interaction with simultaneous measurement of regional cerebral blood flow and electroencephalogram β rhythm in human subjects. Neurosci Lett 275:222–226.

Nichols TE, Holmes AP (2001): Nonparametric permutation tests for functional neuroimaging: a primer with examples. Hum Brain Mapp 15:1–25.

Obrist WD, Sokoloff L, Lassen NA, Lane MH, Butler RN, Feinberg I (1963): Relation of EEG to cerebral blood flow and metabolism in old age. Electroencephalogr Clin Neurophysiol 15:610–619.

Ogawa S, Lee TM, Nayak AS, Glynn P (1990): Oxygenation-sensitive contrast in magnetic resonance image of rodent brain at high magnetic fields. Magn Reson Med 14:68–78.

Pascual-Marqui RD, Michel CM, Lehmann D (1994): Low resolution electromagnetic tomography: a new method for localizing electrical activity in the brain. Int J Psychophysiol 18:49–65.

Pascual-Marqui RD (1999): Review of methods for solving the EEG inverse problem. Int J Bioelectromagnetism 1:75–86.

Pascual-Marqui RD, Lehmann D, Koenig T, Kochi K, Merlo MC, Hell D, Koukkou M (1999): Low resolution brain electromagnetic tomography (LORETA) functional imaging in acute, neuroleptic-naive, first-episode, productive schizophrenia. Psychiatry Res 90:169–179.

Pascual-Marqui RD, Esslen M, Kochi K, Lehmann D (2002): Functional imaging with low resolution brain electromagnetic tomography (LORETA): review, new comparisons, and new validation. Jpn J Clin Neurophysiol 30:81–94.

Phelps ME, Huang SC, Hoffman EJ, Selin C, Sokoloff L, Kuhl DE (1979): Tomographic measurement of local cerebral glucose metabolic rate in humans with (F-18)2-fluoro-2-deoxy-D-glucose: validation of method. Ann Neurol 6:371–388.

Pizzagalli D, Lehmann D, Koenig T, Regard M, Pascual-Marqui RD (2000): Face-elicited ERPs and affective attitude: brain electric microstate and tomography analyses. Clin Neurophysiol 111: 521–531.

Pizzagalli D, Pascual-Marqui RD, Nitschke JB, Oakes TR, Larson CL, Abercrombie HC, Schaefer SM, Koger JV, Benca RM, Davidson RJ (2001): Anterior cingulate activity as a predictor of degree of treatment response in major depression: evidence from brain electrical tomography analysis. Am J Psychiatry 158:405–415.

Pizzagalli DA, Nitschke JB, Oakes TR, Hendrick AM, Horras KA, Larson CL, Abercrombie HC, Schaefer SM, Koger JV, Benca RM, Pascual-Marqui RD, Davidson RJ (2002a): Brain electrical tomography in depression: the importance of symptom severity, anxiety, and melancholic features. Biol Psychiatry 52:73–85.

Pizzagalli DA, Chung M, Oakes TR, Davidson RJ (2002b): Subgenual prefrontal and orbitofrontal cortex dysfunction in melancholia: functional and structural correlates using concurrent EEG/PET measurements and voxel-based MRI morphometry analyses. Psychophysiology 39:S66.

Raichle ME, MacLeod AM, Snyder AZ, Powers WJ, Dusnard DA, Shulman GL (2001): A default mode of brain function. Proc Natl Acad Sci USA 98:676–682.

Sadato N, Nakamura S, Oohashi T, Nishina E, Fuwamoto Y, Waki A, Yonekura Y (1998): Neural networks for generation and suppression of α rhythm: a PET study. Neuroreport 9:893–897.

Schacter DL (1977): EEG θ waves and psychological phenomena: a review and analysis. Biol Psychol 5:47–82.

Schomer DL, Bonmassar G, Lazeyras F, Seeck M, Blum A, Anami K, Schwartz D, Belliveau JW, Ives J (2000): EEG-linked functional magnetic resonance imaging in epilepsy and cognitive neurophysiology. J Clin Neurophysiol 17:43–58.

Seeck M, Lazeyras F, Michel CM, Blanke O, Gericke CA, Ives J, Delavelle J, Golay X, Haenggeli CA, de Tribolet N, Landis T (1998): Non-invasive epileptic focus localization using EEG-triggered functional MRI and electromagnetic tomography. Electroencephalogr Clin Neurophysiol 106:508–512.

Shagass C (1972): Electrical activity of the brain. In: Greenfield NS, Sternbach RA, editors. Handbook of psychophysiology: electrical activity of the brain. New York: Holt, Rinehart, and Winston. p 263–328.

Singh M, Kim S, Kim TS (2003): Correlation between BOLD-fMRI and EEG signal changes in response to visual stimulus frequency in humans. Magn Reson Med 49:108–114.

Sokoloff L, Reivich M, Kennedy C, Des Rosiers MH, Patlak CS, Pettigrew KD, Sakurada O, Shinohara M (1977): The [14C]deoxyglucose method for the measurement of local cerebral glucose utilization: theory, procedure, and normal values in the conscious and anesthetized albino rat. J Neurochem 28:897–916.

Speckman EJ, Elger CE, Altrup U (1993): Neurophysiologic basis of the EEG. In: Wyllie E, editor. The treatment of epilepsy: principles and practices. Philadelphia: Lea and Febiger.

Steriade M, Gloor P, Llinás RR, Lopes de Silva FH, Mesulam MM (1990): Basic mechanisms of cerebral rhythmic activities. Electroencephalogr Clin Neurophysiol 76:481–508.

Talairach J, Tournoux P (1988): Co-planar stereotaxic atlas of the human brain. Stuttgart: Thieme.

Tomarken AJ, Davidson RJ, Wheeler RW, Kinney L (1992): Psychometric properties of resting anterior EEG asymmetry: temporal stability and internal consistency. Psychophysiology 29:576–592.

Towle VL, Bolanos J, Suarez D, Tan K, Grzeszczuk R, Levin DN, Cakmur R, Frank SA, Spire JP (1993): The spatial location of EEG electrodes: locating the best-fitting sphere relative to cortical anatomy. Electroencephalogr Clin Neurophysiol 86:1–6.

Ward DB (2000): Simultaneous inference for fMRI data. In: AlphaSim program documentation for AFNI. Milwaukee: Medical College of Wisconsin. Online at http://aFni.nimh.nih.gov/pub/dist/doc/AlphaSim.pdf

Wiedemann G, Pauli P, Dengler W, Lutzenberger W, Birbaumer N, Buckremer G (1999): Frontal brain asymmetry as a biological substrate of emotions in patients with panic disorders. Arch Gen Psychol 56:78–84.

Worrell GA, Lagerlund TD, Sharbrough FW, Brinkmann BH, Busacker NE, Cicora KM, O'Brien TJ (2000): Localization of the epileptic focus by low-resolution electromagnetic tomography in patients with a lesion demonstrated by MRI. Brain Topogr 12: 273–282.

Worsley KJ, Evans AC, Marrett S, Neelin P (1992): A three-dimensional statistical analysis for CBF activation studies in human brain. J Cereb Blood Flow Metab 12:1040–1042.